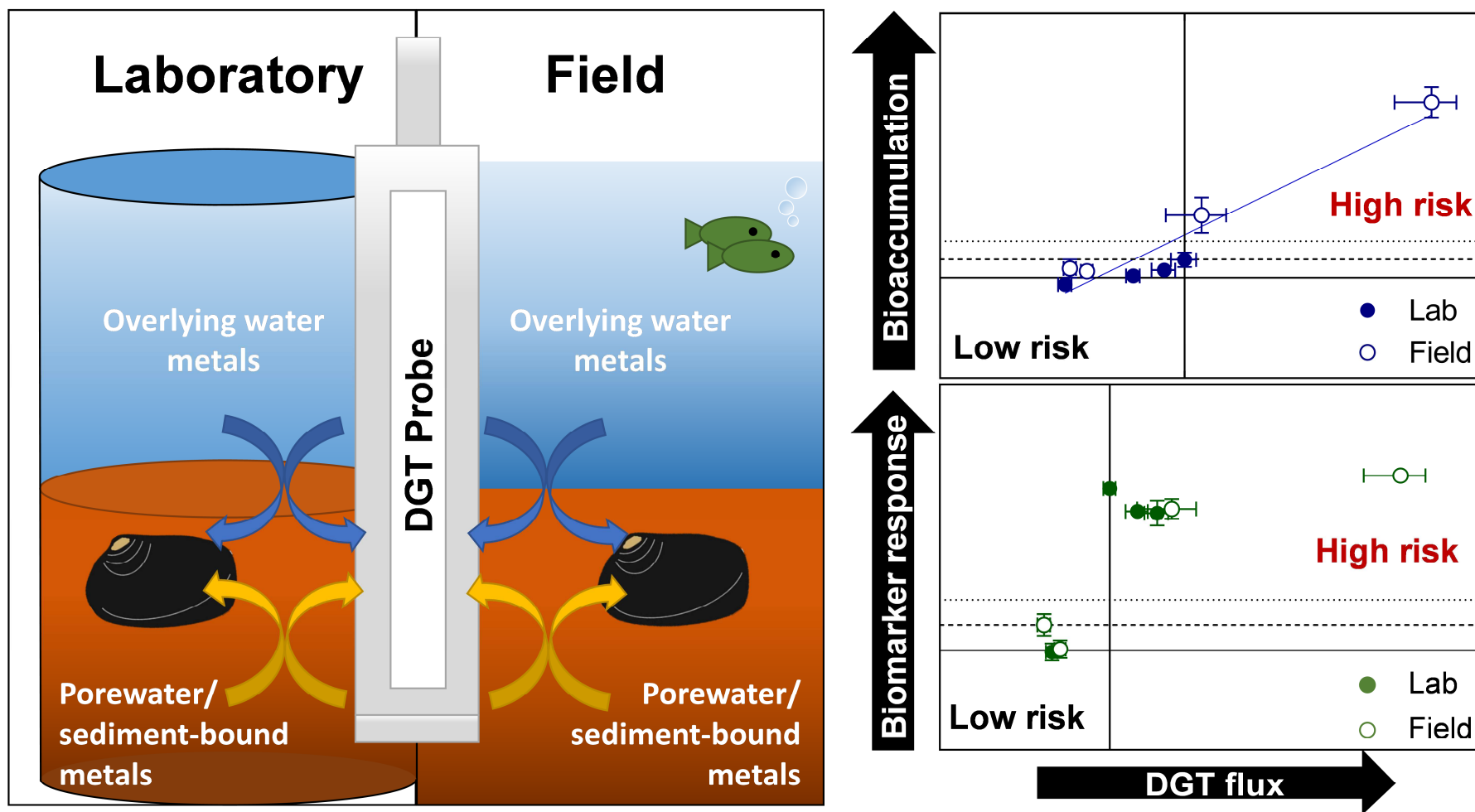


This item is the archived peer-reviewed author-version of:

Field and laboratory evaluation of DGT for predicting metal bioaccumulation and toxicity in the freshwater bivalve *Hyridella australis* exposed to contaminated sediments

Reference:

Amato Elvio, Marasinghe Wadige Chamani P.M., Taylor Anne M., Maher William A., Simpson Stuart L., Jolley Dianne F.- Field and laboratory evaluation of DGT for predicting metal bioaccumulation and toxicity in the freshwater bivalve *Hyridella australis* exposed to contaminated sediments
Environmental pollution - ISSN 0269-7491 - 243:B(2018), p. 862-871
Full text (Publisher's DOI): <https://doi.org/10.1016/J.ENVPOL.2018.09.004>
To cite this reference: <https://hdl.handle.net/10067/1539580151162165141>



1 Running title: Field and laboratory evaluation of DGT for predicting metal bioaccumulation and
2 toxicity in the freshwater bivalve *Hyridella australis* exposed to contaminated sediments

3
4
5 Corresponding author: Elvio Amato

6 Systemic, Physiological and Ecotoxicological Research (SPHERE), Department of Biology,
7 University of Antwerp, Groenenborgerlaan 171, 2020 Antwerp, Belgium

8 tel.: +32 3265 3533; *E-mail address*: elvio.amato@uantwerpen.be

9
10 Rationale: Assessing the risks to ecosystems posed by contaminants is not simple for many
11 environmental matrices. For sediments, there is a need for better techniques for *in situ* assessment of
12 contaminant bioavailability. Analysis of pore waters, acid volatile sulfide (AVS),
13 simultaneously extracted metals (SEM), and organic carbon concentrations are frequently
14 used to evaluate and assist in predicting contaminant bioavailability in sediments. Where
15 concentrations of bioavailable contaminants are assessed to exist near or above guideline
16 levels, bioassays are usually performed to evaluate whether toxic effects may result from
17 contaminant exposure. For metal contaminants, chemical analyses have been useful for
18 predicting metal toxicity in some sediments (e.g. AVS-SEM relationships), however the
19 predictions for more oxidized surface sediments can be quite poor. This is attributed to a
20 broader range of factors influencing metal bioavailability including variability in phases that
21 are easily oxidized or reduced (e.g. AVS and Fe(II)). In addition, laboratory-based bioassays
22 may provide inadequate predictions of metal bioavailability and toxicity due to their inability
23 to adequately replicate field exposure conditions. Thus, techniques capable of providing
24 reliable *in situ* assessments of metal bioavailability and toxicity are needed. In this study, the
25 performance of the diffusive gradients in thin films (DGT) technique for predicting metal
26 bioavailability and sublethal toxicity in sediments was assessed in both the laboratory and
27 field. Strong predictions of bioaccumulation and toxicity were obtained using DGT metal
28 fluxes irrespective of the type of sediment and exposure (i.e., laboratory and field),
29 potentially enabling the derivation of DGT-based threshold values that may be measured *in*
30 *situ* during sediment quality assessments.

31

32 Article Type: Research article

33

34 **Field and laboratory evaluation of DGT for predicting metal bioaccumulation and**
35 **toxicity in the freshwater bivalve *Hyridella australis* exposed to contaminated**
36 **sediments**

37

38 Elvio D. Amato^{†*}, Chamani P.M. Marasinghe Wadige[§], Anne M. Taylor[§], William A. Maher[§], Stuart
39 L. Simpson[†], and Dianne F. Jolley[‡]

40

41 [†] Systemic, Physiological and Ecotoxicological Research (SPHERE), Department of Biology,
42 University of Antwerp, Groenenborgerlaan 171, 2020 Antwerp, Belgium

43

44 [‡] Centre for Environmental Contaminants Research, CSIRO Land and Water, Lucas Heights, NSW
45 2234, Australia

46

47 [‡] School of Chemistry, University of Wollongong, NSW 2522, Australia

48

49 [§] Ecochemistry Laboratory, Institute for Applied Ecology, University of Canberra, Canberra, ACT
50 2601, Australia

51

52 * To whom correspondence may be addressed (elvio.amato@uantwerpen.be)

53 Phone: +32 3265 3533

54 ABSTRACT. The diffusive gradients in thin films (DGT) technique has shown to be a useful
55 tool for predicting metal bioavailability and toxicity in sediments, however, links between
56 DGT measurements and biological responses have often relied on laboratory-based exposures
57 and further field evaluations are required. In this study, DGT probes were deployed in metal-
58 contaminated (Cd, Pb, Zn) sediments to evaluate relationships between bioaccumulation by
59 the freshwater bivalve *Hyridella australis* and DGT-metal fluxes under both laboratory and
60 field conditions. The DGT-metal flux measured across the sediment/water interface (± 1 cm)
61 was useful for predicting significant cadmium and zinc bioaccumulation, irrespective of the
62 type of sediment and exposure. A greater DGT-Zn flux measured in the field was consistent
63 with significantly higher zinc bioaccumulation, highlighting the importance of performing
64 metal bioavailability assessments *in situ*. In addition, DGT fluxes were useful for predicting
65 the potential risk of sub-lethal toxicity (i.e., lipid peroxidation and lysosomal membrane
66 damage). Due to its ability to account for multiple metal exposures, DGT better predicted
67 bioaccumulation and toxicity than particulate metal concentrations in sediments. These
68 results provide further evidence supporting the applicability of the DGT technique as a
69 monitoring tool for sediment quality assessment.

70

71

72 Keywords: metals; bioavailability; biomarkers; bivalves; bioaccumulation; sediment quality
73 assessment

74

75 Major findings:

76 DGT was useful for predicting bioaccumulation and sublethal toxicity to organisms exposed
77 to metal contaminated sediments irrespective of type of sediment and exposure

78

79 1. INTRODUCTION

80 The comparison of total metal concentrations with sediment quality guideline values (SQG)
81 is a common first tier in frameworks used for assessing the risks posed by metal
82 contaminated sediments.^{1,2} When a measured metal concentration exceeds a SQG value, then
83 further investigations are generally required, and often the next step involves considering the
84 bioavailability of the metal contaminants. For metals, analysis of concentrations in pore
85 water, dilute-acid extractable forms, and concentrations of major metal binding phases such
86 as sulfide, organic matter and iron and manganese oxide phases (e.g. through analyses of acid
87 volatile sulfide (AVS), and organic carbon (OC)) are frequently used to evaluate and predict
88 the metal bioavailability.³⁻⁷ Where concentrations of bioavailable metals are determined to
89 exceed SQG values, biological assessment methods are usually used to directly assess the
90 risks of toxicity effects resulting from metal exposure.

91 While use of multiple lines of evidence (LOEs) is an important component of
92 sediment quality assessment,^{2,4,8,9} the requirement to include a LOE for toxicity in
93 assessments adds significantly to assessment costs, and for many environments appropriate
94 toxicity test methods (e.g., relevant species or endpoints) do not yet exist.¹⁰ Consequently,
95 methods that predict the risk of adverse effects comprising physical and chemical
96 measurements continue to be sought to inform the initial phase of assessments.

97 Within surface sediments and the bioturbated zones that are subject to fluctuating
98 dissolved oxygen concentrations, redox-processes strongly influence partitioning of metals
99 among the different solid phases and control metal bioavailability.¹¹⁻¹⁴ Because of the
100 diversity of metal-binding phases,^{4,15} their differing affinities for metals,^{6,12,16-18} and the
101 dynamics of metal-partitioning that alter metal bioavailability and effects to organisms,¹¹⁻¹⁴
102 the creation of a universally applicable method for reliably predicting metal bioavailability in
103 sediments remains elusive.

104 With the intent of providing a method for assessing metal bioavailability that does not
105 need to consider the forms and concentrations of the many metal-binding phases present in
106 the sediments, the diffusive gradient in thin films (DGT) technique is increasingly being
107 applied.¹⁹⁻²⁷ The concept of using DGT to predict metal bioavailability is relatively simple,
108 where higher levels of DGT-labile metals (reported as DGT-induced metal fluxes or
109 concentrations) are taken to indicate a greater risk of metal exposure and adverse effects to
110 benthic invertebrates.^{20,22,23,27} The DGT technique provides time-integrated measurements of
111 some of the metal fractions that are most relevant for bioavailability assessments, such as

112 dissolved metal species present in the pore water, and labile metals that are readily released
113 from the solid phase of the sediment due to weak binding (Zhang et al., 1995).²⁸

114 Another significant challenge for assessments of metal bioavailability is dealing with
115 differences between observations made in the laboratory and those made in the field.^{29,30}
116 While laboratory-based measurements made on sediment collected from the field often
117 provide important information for sediment quality assessments, frequently there is a
118 significant mismatch in exposure conditions between the laboratory and field, and this can
119 lead to considerable differences in the assessment of risk predicted for metal contaminated
120 sediments.^{12,31,32} Metal bioavailability is easily disturbed during sediment sampling and
121 storage prior to testing,^{14,33} and the use of *in situ* techniques such as DGT is expected to
122 provide a more representative measure of concentrations of labile and bioavailable metals
123 existing in the field when compared to measurements made using techniques applied in the
124 laboratory.^{23,26,34}

125 In this study, the ability of the DGT technique to provide measurements that can be
126 used to predict metal bioaccumulation and sub-lethal toxicity to the bivalve *Hyridella*
127 *australis* was tested under laboratory and field conditions. A mining-affected river showing a
128 gradient of metal concentrations was identified as a suitable site for conducting
129 investigations.³⁵ Relationships between biological responses and the DGT-induced metal
130 fluxes were assessed in relation to the application of DGT as a suitable tool for environmental
131 monitoring.

132

133 2. MATERIALS AND METHODS

134 **2.1. General methods.** All glass and plastic-ware used for analyses were new and
135 cleaned by soaking in 10% HNO₃ (v/v) (BDH, AnalaR) for ≥ 24 h, followed by thorough
136 rinsing with ultrapure water (18.2 M Ω -cm). For analytes above trace concentrations, no acid
137 cleaning was undertaken. All chemicals were analytical reagent grade or equivalent analytical
138 purity. Total recoverable metal (TRM) concentrations in sediments were analyzed following
139 low-pressure microwave-assisted aqua regia digestion (3:1 v/v HNO₃:HCl, CEM Mars 5).
140 Dilute-acid extractable metals (AEM, 60 min 1 M HCl digestion) and acid-volatile sulfide
141 (AVS) concentrations were determined according to methods previously described by
142 Simpson et al.³⁶ Metal concentrations in biological tissues were analysed following the
143 procedure described by Baldwin et al.³⁷ Briefly, the soft tissue mass (approximately 0.07 g of
144 tissue or certified reference materials, NIST 1566b, oyster tissue) was freeze-dried and finely
145 ground before microwave-assisted (CEM MDS-2000, USA) extraction in nitric acid

146 (Suprapur® Nitric Acid, Merck, Germany) for 2 min at 630 W, 2 min at 0 W and 45 min at
147 315 W. Discrete overlying water samples were collected for analysis of dissolved metal
148 concentrations. Samples were filtered (0.45 µm) and acidified (1% HNO₃ v/v) immediately
149 after collection in the laboratory or within 24 h when collected from the field. Field samples
150 were collected on days 0 and 28 of the exposure, while laboratory samples were collected on
151 a weekly basis. All digests and water samples were analysed by inductively coupled plasma-
152 atomic emission spectrometry (ICP-AES, Varian 730-ES) and by inductively coupled
153 plasma-mass spectrometry (ICP-MS, Agilent 7500ce). All sediment analyses were performed
154 in triplicate and recoveries of certified material (ERM-CC0018, NIST 1566b) were between
155 90 and 110% of the expected value.

156

157 **2.2. Test media and organisms.** Sediments were collected from four sites along the
158 Molonglo River at different distances from a mining complex located at Captains Flat, near
159 Canberra, ACT, Australia, at a depth comprised between 0 and 10 cm. In each of the sites, a
160 suitable location was identified based on the ease of cages and DGT probes deployment (i.e.,
161 water depth < 1m). Three metal-contaminated and one reference site were identified along
162 the Molonglo River based on past studies.³⁸ The reference sediment was collected at
163 approximately 8 km upstream from the mine (S1), and three contaminated sediments at
164 approximately 45 (S2), 28 (S3), and 9 km (S4) downstream from the mine site (Table 1).
165 Sediment sub-samples for chemical analyses (~500 g) were sieved (2 mm), homogenized and
166 stored in the dark at 4° C until use. River water was collected from each location, filtered
167 (0.45 µm) and stored at room temperature. The freshwater bivalve *Hyridella australis* (5.5 ±
168 0.5 cm) was collected from Nepean River, near Menangle, south-west of Sydney, NSW,
169 Australia.

170

171 **2.3. Bivalve bioassay.** Bioaccumulation in *H. australis* was assessed by exposing
172 bivalves to control (S1) and contaminated sediments (S2, S3, S4) over a period of 28 days.
173 The laboratory bioassay was carried out in plastic aquariums (12 L) containing ~2 kg of
174 sediment and 10 L of filtered (0.45 µm) river water. The exposure media (sediments and
175 waters) were equilibrated for 2 days at room temperature (22-25 °C) before addition of
176 bivalves. Overlying water was aerated using air flow controllers to maintain 80-100% air-
177 saturation during this pre-exposure phase and during the bioassays. In the field bioassay,
178 sediments were placed in plastic mesh cages (35 × 30 × 10 cm³) which allowed sufficient
179 head-space for bivalve movement, adequate water circulation and prevented predation (see

180 Supporting Information (SI)). During the laboratory bioassay, 50% of the overlying water
181 was renewed in all laboratory treatments every 3 days and the bivalves were fed twice a week
182 using unicellular green algae *Nannochloropsis* (Nanno 3600, Instant algae, USA) at 1% (v/w)
183 of total body mass, while no additional food was provided in the field bioassay. Both
184 laboratory and field bioassays were performed in triplicate. At test commencement, six
185 bivalves were placed on the sediment surface of the three treatment replicates (laboratory and
186 field) and allowed to bury. The final bivalve density was approximately 0.8 and 1.2 bivalve/L
187 of sediment for laboratory and field experiments, respectively. In the field bioassay, a mesh
188 lid was placed on the top of the cages, secured in place using plastic cable ties and then
189 placed in the same location as sample collection. Water quality parameters (temperature, pH,
190 dissolved oxygen, and conductivity) were monitored at the beginning, middle and end of test
191 in each of the locations (Table S1 of the SI). After 28 days, organisms were retrieved,
192 depurated in clean fresh water for 24 h, and dissected prior to analysis.

193 Five organisms per replicate were utilized for measuring metal concentrations in
194 whole tissues and one organism for enzymatic assays (biomarker responses). Hepatopancreas
195 tissues were used for total antioxidant capacity (TAOC), lipid peroxidation (MDA), and
196 lysosomal membrane stability assays. Tissues were thawed and homogenized on ice in 500
197 μL of a 5 mM potassium phosphate buffer (0.9% w/v sodium chloride and 0.1% w/v glucose,
198 pH 7.4 (1:5, w/v)), sonicated on ice for 15 s, and centrifuged for 15 min at 4°C. TAOC and
199 MDA assays were carried out on supernatants immediately after tissue processing. Sub-
200 samples of tissue lysates were stored at -80°C for protein analyses that were completed on
201 the following day. The procedures used for TAOC, MDA, and lysosomal membrane stability
202 assays are described elsewhere.³⁹

203

204 **2.4. Diffusive gradients in thin films.** Plastic planar DGT probes (24 cm \times 4 cm \times 0.5
205 cm, with an open window of 1.8 cm \times 15 cm) were purchased from DGT Research
206 (<http://www.dgtresearch.com/>). DGT probes were loaded with Chelex® binding gel (0.4 mm
207 thickness) topped with a polyacrylamide diffusive gel (0.8 mm thickness) and a 0.45 μm pore
208 size (100 μm thickness) polysulfone filter membrane.²⁸ Gel and resin preparation and
209 handling were performed in an AURA SD4 Laminar Flow Cabinet following the procedures
210 recommended by DGT Research (Lancaster, UK). Before deployment, probes were
211 conditioned overnight using a 0.12 M NaCl solution of ultrapure water continuously bubbled
212 with nitrogen gas, then maintained under an inert gas atmosphere until deployment (<4 h).

213 In the laboratory bioassays, one DGT probe was deployed in each of the three test
214 chamber replicates. In the field, three DGT probes were deployed directly in the sediment
215 near the cages used for the *in situ* bioassay (height limitations prevented probe deployment
216 within cages). DGT probes were deployed in two separate events, in the first and third week
217 of the bioassays (laboratory deployment: day 4 and 16 for sediments S1 and S2 and day 2 and
218 16 for sediments S3 and S4; field deployment: day 7 and 21 for sediments S1 and S3 and day
219 2 and 16 for sediments S2 and S4). After probe retrieval, a hole in the sediment bed was
220 generally observed. This unlikely caused any significant disturbance in the sediment or in the
221 overlying water. In the second deployment, care was taken to deploy probes at an adequate
222 distance from the previous deployment point (~10-20 cm).

223 After a 24-h deployment, probes were removed and thoroughly rinsed with ultrapure
224 water, placed in acid-washed plastic bags and stored at 4°C until analysis. Probes were
225 disassembled and the Chelex-resin sliced at 1 and 3 cm above the sediment water interface
226 (SWI), and 1, 2 and 4 cm below the SWI. In laboratory chambers, the maximum depth
227 achievable for DGT measurements was -3 cm, and when necessary, the slicing procedure was
228 adjusted according to the available depth (-2 and -4 cm for S1 and S4, respectively - first
229 deployment). Resin slices were extracted with 1 M HNO₃, diluted 10-fold with ultrapure
230 water and analysed by ICP-MS (Agilent 7500ce). The measured concentration in the extract
231 was used to calculate the mass per unit area ($\mu\text{g}/\text{m}^2$) in the resin gel and divided by the
232 deployment time to obtain DGT-labile metal fluxes ($\mu\text{g}/\text{h}/\text{m}^2$). For quality assurance,
233 laboratory and field blank probes were analyzed; blank probes were exposed to the air and
234 then rinsed with the same ultrapure water used for cleaning probes upon retrieval.

235
236 **2.5. Data analysis.** Statistical analyses were performed using the software R 3.1.2
237 ($\times 64$). Differences in metal bioaccumulation rates between organisms exposed to different
238 treatments (S1, S2, S3, S4) and exposure conditions (laboratory and field) were investigated
239 using two-way analysis of variance (ANOVA) with interactions between type of sediment
240 and type of exposure, followed by Tukey's test. Data were tested for normality of residuals
241 distribution (Shapiro-Wilk's test) and for homogeneity of variance (Levene test) prior to
242 hypothesis testing. When the data did not follow a normal distribution, Kruskal-Wallis test
243 followed by Wilcoxon-Mann-Whitney test were performed. Unless otherwise stated, the
244 level of significance α was 0.05. To account for the varying toxicity expected to be caused by
245 the different metals, exposure concentrations and fluxes (dissolved metal concentrations,
246 DGT fluxes and AEM concentrations) were converted to quotients by dividing each metal

247 exposure concentration or flux by its corresponding guideline value,⁴⁰ and then summing the
248 quotients in the case of more than one metal. For AEM, the guideline value was the
249 corresponding SQG value² and, for DGT fluxes and dissolved metal concentrations, the
250 guideline values were the corresponding water quality guidelines values (WQG).⁴¹ According
251 to this approach, DGT fluxes, dissolved metal concentrations, and AEM concentrations were
252 converted to WQG value-based DGT_{SWI} fluxes ($DGT_{WQG-SWI}$), WQG value-based toxic units
253 (TU), and SQG value-based quotients (SQG-Q), respectively.

254

255 **3. RESULTS AND DISCUSSION**

256 **3.1. Sediment chemical and physical properties.** General physico-chemical
257 characteristics (particle size, TOC, AVS) and TRM and AEM concentrations (Cd, Pb and Zn)
258 in field-collected sediment are shown in Table 1, with a greater range of metal and metalloid
259 concentrations shown in Table S1 of the Supporting Information (SI). All sediments collected
260 from sites located downstream of the mine site exhibited significant metal contamination,
261 with SQG values being exceeded for lead in sediment S4, cadmium in S2 and S4, and zinc in
262 S2, S3 and S4 (Table 1). In the reference sediment S1, metal concentrations were well below
263 the SQG values (Table S2 of the SI). TOC concentrations were 1.4, 1.6, 4.3, 1.7% for site S1,
264 S2, S3 and S4, respectively. AVS concentrations of 1.7 ± 0.6 and 6.6 ± 1.0 $\mu\text{mol/g}$ were
265 measured in sediment S2 and S4, respectively, whereas for S1 and S3, concentrations were
266 < 0.5 $\mu\text{mol/g}$ (Table 1). The more labile sulfide phases (e.g. FeS and MnS) that comprise
267 much of the AVS strongly influence the metal speciation and bioavailability in sediments as
268 they react to form insoluble metal-sulfide compounds. AVS and simultaneously-extractable
269 metal (SEM) concentrations (SEM is equivalent to 1 M HCl AEM) are used by equilibrium
270 partitioning approaches (EqP) to identify increased environmental risk when molar
271 concentrations of SEM exceed AVS in the sediment, where higher organic carbon (OC)
272 concentrations also lower the bioavailability of SEM in excess of AVS (Burgess et al. 2013).⁵
273 Based on calculations of SEM-AVS and $(SEM-AVS)/f_{OC}$ (where f_{OC} is the fraction of OC),
274 all contaminated sediments (S2, S3 and S4) indicated potential risk of toxicity to benthic
275 organisms (Table 1).

276

277 **3.2. Metal profiles in sediments and overlying waters by DGT.** Concentrations in
278 blank extracts from DGT-probes were generally low for all metals except for zinc. The blank
279 Cu, Mn, Ni and Pb concentrations were estimated to contribute an equivalent flux < 0.2
280 $\mu\text{g/h/m}^2$, whereas cadmium and lead contributed < 0.005 and < 4 $\mu\text{g/h/m}^2$, respectively.

281 Significant zinc contamination was found and estimated to contribute for an equivalent flux
282 of $63\pm 40 \mu\text{g}/\text{h}/\text{m}^2$ (mean \pm SD).

283 Fe(II) and Mn(II) profiles in sediments and overlying waters are shown in Figure 1.
284 Increasing DGT-Fe and -Mn fluxes observed within 2 cm below the SWI indicated the
285 presence of the sub-oxic transition zone, where both bacterial-assisted reduction of insoluble
286 iron and manganese oxyhydroxides phases to soluble reduced forms (Fe(II) and Mn(II)), and
287 the oxidation of iron and manganese sulfides to oxyhydroxides, may take place.^{22,23,42}

288 Small but consistent variations in DGT-Cu profiles measured in the laboratory may
289 indicate potential mobilization of this metal at approximately 0.5 cm below the SWI (Figure
290 1). Similarly, release of DGT-Pb was also observed at this depth in sediment S4. This was
291 attributed to the reductive dissolution of the iron and manganese solid phases,^{22,43} and the
292 oxidation of metal sulfides.^{44,45} The peaks in DGT metal profiles may also be associated with
293 locations with the greatest rate of degradation of organic matter, resulting in an
294 accompanying release of metals to the pore water.^{46,47}

295

296 **3.3. Differences in DGT-measured metal fluxes between laboratory and field**

297 **deployments.** The location within the sediment profiles and magnitude of the iron and
298 manganese fluxes measured by DGT were similar for laboratory and field deployments for
299 sediments S1 and S2, whereas sediment S3 showed greater iron and manganese fluxes in
300 field deployments and sediment S4 greater iron fluxes in laboratory deployments (Figure 1,
301 with greater detail in Figure S1 of the SI). In sediment S3, DGT-Fe fluxes in the sediment
302 pore waters of the field deployments were approximately 5 times greater than those from the
303 laboratory. Similarly, greater DGT-Mn fluxes were measured in sediment S3 during field
304 deployments in both the sediment pore water (630 ± 370 and $1900\pm 440 \mu\text{g}/\text{h}/\text{m}^2$, for
305 laboratory and field deployments, respectively) and overlying water (16 ± 10 and 840 ± 100
306 $\mu\text{g}/\text{h}/\text{m}^2$, for laboratory and field deployments, respectively). This may be due to the higher
307 oxygen concentrations measured in the overlying water of the laboratory-exposed sediments
308 (i.e., oxygen saturation in the field was ~ 50 - 60% , Table S2 of the SI), which may have
309 resulted in greater rates of oxidation of Fe(II) and Mn(II) in both the pore water and
310 overlying water.^{14,33,48} As a consequence, porewater iron and manganese concentrations in
311 the laboratory-exposed sediment may have become lower due to a significantly greater rate of
312 precipitation of iron oxyhydroxides occurring as a result of oxygen penetration in the
313 sediment.⁴² A different trend was observed for iron in sediment S4, where greater DGT-Fe

314 fluxes were measured in the sediment pore waters under laboratory conditions (7600±2600
315 and 2800±2200 µg/h/m² for laboratory and field deployments, respectively).

316 Despite the difference in particulate zinc concentrations (Table 1), similar DGT-Zn
317 fluxes were measured in all laboratory-exposed sediments. In contrast, considerable
318 differences between sites were observed in the field, with a 10 and 100-fold greater DGT-Zn
319 flux measured in sediment S3 and S4, respectively, as compared to S1 and S2 (Figure 1). The
320 DGT-Zn flux was greater in laboratory deployments for sediment S2 (48-53 and 97-209
321 µg/h/m² for field and laboratory deployments, respectively) and in field deployments for
322 sediment S1 (36-51 and 53-87 µg/h/m² for laboratory and field deployments, respectively).

323 DGT-Cu and Pb fluxes appeared to be slightly lower in field deployments, except for
324 sediment S4 which exhibited a greater DGT-Cu flux under field conditions (Figure 1). DGT-
325 Ni fluxes were similar between laboratory and field deployments in sediments S3 and S2, but
326 considerably greater in sediment S4 (and S1 in the sediment pore water) in the field. DGT-Cd
327 fluxes were also considerably larger in field deployments for sediment S4 (2.4 µg/h/m²),
328 whereas in the other sediments fluxes were <0.3 µg/h/m².

329 Overall, little differences in metal fluxes measured by DGT were observed between
330 laboratory and field deployments in the less contaminated sediments (S1 and S2), and
331 considerably greater fluxes were observed for Cd, Ni and Zn for the two more contaminated
332 sites located the nearer to the mine site (S3 and S4).

333

334 **3.4. Metal bioaccumulation by the bivalve.** Significant bioaccumulation in *H.*
335 *australis* was observed only for cadmium and zinc. In the laboratory, cadmium
336 bioaccumulation in bivalves exposed to contaminated sediments (S2, S3, S4) exceeded that
337 of organisms exposed to the reference sediment (S1) (p<0.05) (Table 1), consistent with the
338 higher particulate cadmium concentrations found in the contaminated sediments (Table 1).
339 Under field conditions, only bivalves exposed to S4 exhibited higher cadmium
340 bioaccumulation than organisms exposed to the reference site (S1) (p<0.001), consistent with
341 S4 having the highest level of cadmium contamination. When comparing cadmium tissue
342 concentrations of bivalves exposed to laboratory vs field conditions, bioaccumulation of
343 bivalves deployed in S4 in the field was considerably greater than that of bivalves exposed to
344 the same sediment under laboratory conditions (p<0.001), while, in contrast, lower cadmium
345 bioaccumulation was observed in field-deployed bivalves for site S2 and S3 (p<0.01) (Figure
346 S2 of the SI). These results indicate a significant difference in cadmium exposure between
347 laboratory and field exposure.

348 Despite the considerable difference in zinc concentrations found between reference
349 and contaminated sediments (Table 1), no significant differences ($p>0.05$) in zinc
350 bioaccumulation were observed between bivalves exposed to these sediments under
351 laboratory conditions. AEM/TRM ratios between 0.87-0.89 were measured in contaminated
352 sediments, suggesting that only a minor but fairly constant portion of sediment-bound zinc
353 was likely to be in highly mineralized and more inert forms. The similar level of zinc
354 bioaccumulation measured in all the laboratory exposures suggests that zinc tissue
355 concentrations in *H. australis* were not being influenced by the different particulate zinc
356 concentrations. However, significantly greater zinc bioaccumulation was observed in field
357 exposures at sites S3 and S4 ($p<0.001$) compared to the reference site. As the sediments in
358 the respective field and laboratory exposures were the same, this indicates that other factors
359 were influencing the bioaccumulation of zinc. This was confirmed by the strong correlations
360 between dissolved zinc concentrations in overlying waters and bioaccumulation of this metal
361 (Figure 2, additional regression parameters provided in Table S3), indicating a strong
362 contribution from the dissolved phase to the exposure of this bivalve.

363

364 **3.5. Use of the DGT fluxes for assessing potential for metal bioaccumulation.**

365 The magnitude of the DGT-Cd and -Zn fluxes (average of first and second deployments)
366 were generally consistent with the magnitude of their bioaccumulation by *H. australis*
367 exposed to different treatments (S1, S2, S3, S4) and test conditions (laboratory and field).
368 Generally low DGT-Cu and DGT-Pb fluxes measured in reference (S1) and contaminated
369 (S2, S3, S4) sediments were consistent with low copper and lead bioaccumulation in bivalves
370 exposed to these sediments (Figure 1, Table 1). In the field, the considerably larger DGT-Cd
371 fluxes in S4, and DGT-Zn fluxes in S3 and S4, were consistent with significantly higher
372 concentrations of cadmium and zinc accumulated in the bivalve tissues (Figures 2 and S3).
373 For less contaminated sediments S1 and S2, DGT-metal fluxes in laboratory and field
374 deployments were low (<0.1 , <1.5 , <2 and $<200 \mu\text{g}/\text{h}/\text{m}^2$ for Cu, Cd, Pb and Zn,
375 respectively) (Figure 1) and within the range of DGT-metal fluxes measured in sediments
376 shown to cause low toxicity to the amphipod *Melita plumulosa* and low bioaccumulation to
377 the bivalve *Tellina deltoidalis*.^{22,23,42}

378 The DGT flux measurements in the overlying water, and sediment pore water near the
379 SWI and in deeper sediments, provide information on metal exposure routes for the bivalve.
380 Previous studies have shown that DGT-metal fluxes measured at the SWI were useful for
381 predicting toxicity to the amphipod *M. plumulosa*²² and bioaccumulation and toxicity to the

382 bivalve *T. deltoidalis*.^{20,23,42} *H. australis* is a filter-feeding bivalve which has been shown to
383 accumulate metals in response to exposure to contaminated sediments.⁴⁹⁻⁵¹ Although
384 exposure pathways for metal uptake have not been directly investigated for this species,
385 previous studies indicated that exposure to the dissolved phase may be a major route of
386 uptake for *H. australis*.^{49,50} Since the bivalve may be exposed to metals present in the
387 overlying waters and pore waters (including resupply of DGT-labile metals from the
388 sediment phase that are not measured by direct porewater analyses), relationships between
389 bioaccumulation and DGT-Cd and DGT-Zn fluxes were investigated using fluxes measured
390 in (i) the water column (between 0 and 3 cm above the SWI, DGT_{OLW}), (ii) at the SWI (± 1
391 cm, DGT_{SWI}) and (iii) in the pore water (between 0 and -3 or -4 cm below the SWI, DGT_{SED})
392 (Figure S3, additional regression parameters provided in Table S3 of the SI).

393 Strong correlations were found between bioaccumulation and both the $\log_{10} DGT_{OLW}$ -
394 Zn flux ($R = 0.964$) and the $\log_{10} DGT_{SWI}$ -Zn flux ($R = 0.951$), whereas weaker correlations
395 were obtained using corresponding fluxes measured in the sediment pore water ($R = 0.820$)
396 (Figure S3 of the SI). These strong correlations are consistent with exposure to dissolved zinc
397 being the major route for bioaccumulation for this bivalve. In a companion paper,
398 Marasinghe Wadige et al.⁵² showed that the majority of zinc accumulated in the organisms
399 investigated in this study was found in the gills. Linear regression analysis obtained by
400 plotting zinc concentrations measured in the gills against the $\log_{10} DGT_{SWI}$ -Zn, $\log_{10} DGT_{OLW}$ -
401 Zn, and $\log_{10} DGT_{SED}$ -Zn flux indicated strong correlation between DGT measurements and
402 bioaccumulation in gills (Figure S4, additional regression parameters provided in Table S3 of
403 the SI). The better fit obtained using DGT fluxes measured at the SWI ($R = 0.960$) and in the
404 overlying water ($R = 0.941$) suggested a predominant exposure of *H. australis* to DGT-labile
405 zinc present in the overlying water rather than DGT-labile zinc released in the bulk sediment
406 ($R = 0.883$).

407 Poor relationships were found between cadmium bioaccumulation and DGT-Cd
408 measurements, likely due to the smaller range of cadmium concentrations measured in
409 sediments and overlying water, which resulted in relatively low bioaccumulation of cadmium
410 for all bivalves except for those exposed to S4 in the field (Figure S2 of the SI).

411 Overall, predictions of bioaccumulation obtained using the DGT-Zn flux measured in
412 the overlying water and at the SWI were very similar. Previous research has shown that the
413 DGT-metal flux measured at the SWI was useful for predicting bioaccumulation and toxic
414 effects to benthic organisms.^{22,23,42} To allow the comparison with this work, only DGT

415 measurements performed at the SWI (± 1 cm) will be further discussed for the interpretation
416 of bioaccumulation and toxic effects to *H. australis*.

417

418 **3.6. Comparison between predictions of zinc bioaccumulation based on**
419 **exposure measurements to particulate zinc in sediments, dissolved zinc in**
420 **overlying water, and the DGT-Zn flux.** Due to the overall low bioaccumulation of
421 cadmium, copper, and lead observed in exposed organisms (Table 1), comparisons of metal
422 exposure and bioaccumulation are discussed only for zinc.

423 Total and dilute-acid extractable zinc concentrations (TR-Zn and AE-Zn) were highly
424 correlated, and therefore the exposure from particulate zinc only considers AE-Zn. The AE-
425 Zn concentrations provided strong predictions of bioaccumulation in bivalves in the separate
426 laboratory ($R = 0.965$) and field ($R = 0.910$) exposures (Figure 2). However, when laboratory
427 and field data were analyzed together, AE-Zn concentrations provided poor predictions of
428 bioaccumulation ($R = 0.624$) (Figure 2). This was likely due to a much greater contribution of
429 dissolved zinc to the exposure of organisms in the field, as indicated by dissolved zinc
430 concentrations and the DGT measurements performed at the SWI and in the overlying water
431 (Figures 2 and S2 of the SI).

432 Among the three approaches used to evaluate the risk of excessive zinc
433 bioaccumulation in *H. australis*, the best predictions were obtained using the \log_{10} DGT_{SWI}-Zn
434 flux ($R = 0.951$) and dissolved zinc concentrations ($R = 0.940$), whereas poor predictions
435 were obtained using AEM concentrations ($R = 0.624$). TRM and AEM concentrations were
436 measured in sub-samples collected in the field. While TRM concentrations were not expected
437 to change between laboratory and field experiments, AEM may have differed due to
438 alteration of the sediment chemical properties caused by sediment collection and
439 homogenization.³³ Thus, such artifacts may have potentially affected the exposure of
440 organisms to particulate zinc. However, both the DGT flux and dissolved concentrations
441 indicated strong links between dissolved zinc and bioaccumulation (Figures 2 and S2 of the
442 SI), suggesting that bivalves were mainly exposed to forms of zinc that were not inherently
443 measured by the AEM method. This is consistent with the filter-feeding behavior of the
444 organisms and also supported by the greatest concentration of metals found in gills which
445 was accurately predicted by the DGT_{SWI}-Zn and the DGT_{OLW}-Zn flux (Figure S4 of the SI).

446 In a previous study, we used a quadrant approach to assist with the identification of
447 DGT-based threshold values for predicting significant risk of metal bioaccumulation in
448 bivalves.²³ This approach allowed identification of the DGT_{SWI}-Zn flux above which

449 bioaccumulation of zinc in bivalves was consistently higher than the mean metal
450 concentration measured in control organisms plus 1 standard deviation (s) (Figure 2). Based
451 on this approach, both dissolved metal concentrations and the DGT_{SWI} -Zn flux clearly
452 distinguished sites and exposures that caused significant bioaccumulation (i.e.,
453 bioaccumulation > mean metal concentration measured in control organisms plus 1 s) (top-
454 left quadrant) from those that did not cause significant bioaccumulation (bottom-right
455 quadrant). In contrast, AEM or TRM concentrations did not provide a clear separation
456 between sites and exposures that caused different bioaccumulation (figures not shown).
457 Based on the quadrant approach, a DGT_{SWI} -Zn flux of $220 \mu\text{g}/\text{h}/\text{m}^2$ was found suitable as a
458 potential threshold value for predicting the risk of significant bioaccumulation of zinc (e.g.,
459 low risk when DGT-Zn flux was below $220 \mu\text{g}/\text{h}/\text{m}^2$), irrespective of sediment type and
460 exposure (Figure 2). This level of DGT-Zn flux was slightly greater than that found in
461 previous work indicating significant risk of bioaccumulation of zinc in the epibenthic bivalve
462 *Tellina deltoidalis* in the range $130\text{-}160 \mu\text{g}/\text{h}/\text{m}^2$.^{23,42} Considering the difference in size and
463 exposure routes of the species investigated, DGT predictions of zinc bioaccumulation
464 obtained in the different studies fell in a relatively narrow range, suggesting that the DGT
465 technique could be used for deriving useful threshold values for sediment quality assessment
466 purposes.

467

468 **3.7. Use of DGT flux data to predict toxicity.** In the companion paper, Marasinghe
469 Wadige et al.⁵² performed a series of enzymatic assays and sub-cellular distribution analysis
470 to evaluate sub-lethal effects induced by the varying sediment types and exposures. In
471 particular, significantly reduced lysosomal membrane stability, higher lipid peroxidation
472 (malondialdehyde (MDA)), and lower total antioxidant capacity (TAOC) were found in
473 organisms exposed to contaminated sediments in comparison to organisms exposed to
474 reference sediments. In the present study, these data were combined with AEM
475 concentrations, dissolved metal concentrations (dM) measured in discrete overlying water
476 samples, and the DGT flux in order to investigate dose-response relationships useful for
477 predicting the observed toxic effects. The performance of the three different techniques for
478 assessing the potential risk of sub-lethal toxicity associated with metal exposure was assessed
479 using the quadrant approach described in the previous section. To account for the varying
480 toxicity expected to be caused by the different metals, dissolved metal concentrations,
481 DGT_{SWI} fluxes and AEM concentrations were converted to WQG value-based toxic units
482 (TU), WQG value-based DGT_{SWI} fluxes ($DGT_{WQG-SWI}$), and SQG value-based quotients

483 (SQG-Q), respectively (details provided in the Materials and Methods section). Based on the
484 guideline quotient approach, onset of significantly lower lysosomal stability was similarly
485 predicted by quotients based on AEM and $DGT_{WQG-SWI}$ fluxes (Figure 3), although the SQG-
486 Q plot featured a data point in the top-left quadrant, indicating a weaker ability of this
487 approach to separate toxic from non-toxic exposures. No significant trends were observed for
488 TOAC, most likely due to the overall little differences in effects detected by this biomarker
489 among the various exposures (Figure 3). TAOC appeared to decrease in response to
490 increasing SQG-Qs and $DGT_{WQG-SWI}$ fluxes, consistently with increased oxidative stress
491 induced by exposure to metals.^{49,51,53} However, slightly lower TAOC was observed in
492 laboratory-exposed organisms compared to field-exposed organisms,⁵² in contrast with the
493 greater exposure to cadmium and zinc in the field (S3 and S4) predicted by the DGT flux and
494 dissolved concentrations (Figures 1, 2 and S3). As a consequence, uncertainty still remain as
495 to whether changes in TAOC may have been linked to exposure to metals or due to other
496 factors.

497 Lipid peroxidation generally increased with increasing SQG-Qs, TUs, and $DGT_{WQG-SWI}$
498 fluxes (Figure 3), however, according to the quadrant approach, no suitable threshold
499 values could be derived using SQG-Qs and TUs. In contrast, the $DGT_{WQG-SWI}$ flux was useful
500 for separating toxic from non-toxic exposures (Figure 3), although a greater toxicity range
501 may have contributed to a better evaluation of the performance of the three different
502 approaches. $DGT_{WQG-SWI}$ fluxes of 9 and 19 $\mu\text{g}_{WQG}/\text{h}/\text{m}^2$ were identified as suitable threshold
503 values for predicting potential risk of lysosomal destabilization and lipid peroxidation,
504 respectively (Figure 3). These values were of similar magnitude to those indicating potential
505 sub-lethal effects to the amphipod *M. plumulosa* for a $DGT_{WQG-SWI}$ flux greater than 17
506 $\mu\text{g}_{WQG}/\text{h}/\text{m}^2$.²²

507

508 4. CONCLUSIONS

509 Overall, the findings of this study indicate that differences between laboratory and field-
510 based bioassays may result in significantly different predictions of risk due to the inability of
511 laboratory bioassays to recreate realistic exposure conditions. Among the three approaches
512 investigated, the DGT-metal flux and dissolved metal concentrations appeared to provide
513 more reliable predictions of metal exposure of *H. australis*, consistent with the filter feeding
514 behavior of this bivalve. While measuring dissolved metal concentrations in discrete water
515 samples is less labor-intensive than performing DGT measurements, for deposit-feeding
516 organisms such as *T. deltoidalis*, exposure to particulate metals and release of metals at the

517 SWI may significantly contribute to benthic organisms' exposure.²³ Therefore, measurements
518 that may be representative of both exposure to sediment and overlying water, such as DGT,
519 could be useful for a more comprehensive evaluation of the risk posed by metal contaminants
520 to benthic organisms. Strong relationships between the DGT-Zn flux and bioaccumulation
521 were found irrespective of the different chemical and physical properties of the sediments
522 (Table 1) and type of exposure (laboratory and field). Similarly, the $DGT_{WQG-SWI}$ flux was
523 also useful for predicting sub-lethal effects to the bivalve. The DGT-based threshold values
524 identified in this study may act as possible threshold values above which the risk of zinc
525 bioaccumulation and sub-lethal effects caused by exposure to metal mixtures may be
526 expected to become significant. These results suggest that the DGT technique has the
527 potential to be used as a tool for *in situ* monitoring of metal bioavailability in contaminated
528 sediments, and may improve this line of evidence when applied for sediment quality and risk
529 assessment purposes.

530
531
532

533 ■ ACKNOWLEDGMENTS

534 Dr James Dawber is thanked for data analysis support. The authors acknowledge the financial
535 support of the NSW Environmental Trust (Research Project APP2010-RD-0177), the
536 University of Wollongong (scholarship for Elvio Amato), and CSIRO Land and Water.
537 Chamani Marasinghe Wadige was funded by the Richard Norris Freshwater Ecology
538 scholarship.

539
540

541 Supporting information

542 Plastic cages (2 cm mesh) used to for the *in situ* bioassay. Metal concentrations in the test
543 sediments. Water quality parameters measured during the field bioassay.

544 Comparison between DGT-Fe and -Mn vertical profiles measured in the first and second
545 deployment in laboratory-exposed sediments. Relationships between bioaccumulation and the
546 DGT-Zn flux measured in the overlying water (OLW) (between 0 and 3 cm above the SWI),
547 at the SWI (± 1 cm), and in the pore water (SED) between 0 and -2.5 and between 0 and -3
548 cm below the SWI for laboratory and field deployment, respectively. Relationships between
549 bioaccumulation and the DGT-Cd flux measured in the overlying water (OLW) (between 0

550 and 3 cm above SWI), at the SWI (± 1 cm), and in the pore water (SED) between 0 and 2.5
551 and between 0 and 3 cm below the SWI for laboratory and field deployment, respectively.
552 Relationships between bioaccumulation in the gills of *H. australis* and the DGT-Zn flux
553 measured in the overlying water (OLW) (between 0 and 3 cm above the SWI), at the SWI (\pm
554 1 cm), and in the pore water (SED) between 0 and 2.5 and between 0 and 3 cm below the
555 SWI for laboratory and field deployment, respectively.

556 ■ REFERENCES

- 557 (1) Bay S. M.; Ritter K. J.; Vidal-Dorsch D. E.; Field L. J. Comparison of National and
558 Regional Sediment Quality Guidelines for Classifying Sediment Toxicity in California.
559 *Integr. Environ. Assess. Manag.* **2012**, *8*, 597–609.
- 560 (2) Simpson, S. L.; Batley, G. E. *Sediment Quality Assessment: A Practical Guide*; CSIRO
561 Publishing: Carlton, Vic, 2016.
- 562 (3) Di Toro, D. M.; McGrath, J. A.; Hansen, D. J.; Berry, W. J.; Paquin, P. R.; Mathew, R.;
563 Wu, K. B.; Santore, R. C. Predicting Sediment Metal Toxicity Using a Sediment Biotic
564 Ligand Model: Methodology and Initial Application. *Environ. Toxicol. Chem.* **2005**, *24*,
565 2410–2427.
- 566 (4) Simpson, S. L.; Batley, G. E. Predicting Metal Toxicity in Sediments: A Critique of
567 Current Approaches. *Integr. Environ. Assess. Manag.* **2007**, *3*, 18–31.
- 568 (5) Burgess, R. M.; Berry, W. J.; Mount, D. R.; Di Toro, D. M. Mechanistic Sediment
569 Quality Guidelines Based on Contaminant Bioavailability: Equilibrium Partitioning
570 Sediment Benchmarks. *Environ. Toxicol. Chem.* **2013**, *32*, 102–114.
- 571 (6) Campana, O.; Simpson, S. L.; Spadaro, D. A.; Blasco, J. Sub-Lethal Effects of Copper
572 to Benthic Invertebrates Explained by Sediment Properties and Dietary Exposure.
573 *Environ. Sci. Technol.* **2012**, *46*, 6835–6842.
- 574 (7) Schlekot C. E.; Garman E. R.; Vangheluwe M. LU; Burton G. A. Development of a
575 Bioavailability-based Risk Assessment Approach for Nickel in Freshwater Sediments.
576 *Integr. Environ. Assess. Manag.* **2016**, *12*, 735–746.
- 577 (8) Bay S. M.; Weisberg S. B. Framework for Interpreting Sediment Quality Triad Data.
578 *Integr. Environ. Assess. Manag.* **2010**, *8*, 589–596.
- 579 (9) Chapman, P. M. Determining When Contamination Is Pollution — Weight of Evidence
580 Determinations for Sediments and Effluents. *Environ. Int.* **2007**, *33*, 492–501.
- 581 (10) Simpson, S. L.; Campana, O.; Ho, K. T. Chapter 7 – Sediment Toxicity Testing; *Mar.*
582 *Ecotox.*, 2017; pp 199–237.

- 583 (11) Simpson, S. L.; Ward, D.; Strom, D.; Jolley, D. F. Oxidation of Acid-Volatile Sulfide in
584 Surface Sediments Increases the Release and Toxicity of Copper to the Benthic
585 Amphipod *Melita plumulosa*. *Chemosphere* **2012**, *88*, 953–961.
- 586 (12) Costello, D. M.; Hammerschmidt, C. R.; Burton, G. A. Copper Sediment Toxicity and
587 Partitioning during Oxidation in a Flow-Through Flume. *Environ. Sci. Technol.* **2015**,
588 *49* (11), 6926–6933.
- 589 (13) Costello, D. M.; Hammerschmidt, C. R.; Burton, G. A. Nickel Partitioning and Toxicity
590 in Sediment during Aging: Variation in Toxicity Related to Stability of Metal
591 Partitioning. *Environ. Sci. Technol.* **2016**, *50*, 11337–11345.
- 592 (14) Remaili, T. M.; Simpson, S. L.; Amato, E. D.; Spadaro, D. A.; Jarolimek, C. V.; Jolley,
593 D. F. The Impact of Sediment Bioturbation by Secondary Organisms on Metal
594 Bioavailability, Bioaccumulation and Toxicity to Target Organisms in Benthic
595 Bioassays: Implications for Sediment Quality Assessment. *Environ. Pollut.* **2016**, *208*,
596 590–599.
- 597 (15) Chapman, P. M.; Wang, F.; Janssen, C.; Persoone, G.; Allen, H. E. Ecotoxicology of
598 Metals in Aquatic Sediments: Binding and Release, Bioavailability, Risk Assessment,
599 and Remediation. *Can. J. Fish. Aquat. Sci.* **1998**, *55*, 2221–2243.
- 600 (16) Costello, D. M.; Burton, G. A.; Hammerschmidt, C. R.; Rogevich, E. C.; Schlekot, C. E.
601 Nickel Phase Partitioning and Toxicity in Field-Deployed Sediments. *Environ. Sci.*
602 *Technol.* **2011**, *45*, 5798–5805.
- 603 (17) Strom, D.; Simpson, S. L.; Batley, G. E.; Jolley, D. F. The Influence of Sediment
604 Particle Size and Organic Carbon on Toxicity of Copper to Benthic Invertebrates in
605 Oxidic/Suboxic Surface Sediments. *Environ. Toxicol. Chem.* **2011**.
- 606 (18) Besser J. M.; Brumbaugh W. G.; Ingersoll C. G.; Ivey C. D.; Kunz James L.; Kemble N.
607 E.; Schlekot C. E.; Garman E. R. Chronic Toxicity of Nickel-spiked Freshwater
608 Sediments: Variation in Toxicity among Eight Invertebrate Taxa and Eight Sediments.
609 *Environ. Toxicol. Chem.* **2013**, *32*, 2495–2506.
- 610 (19) Roulier, J. L.; Tusseau-Vuillemin, M. H.; Coquery, M.; Geffard, O.; Garric, J.
611 Measurement of Dynamic Mobilization of Trace Metals in Sediments Using DGT and

- 612 Comparison with Bioaccumulation In *Chironomus riparius*: First Results of an
613 Experimental Study. *Chemosphere* **2008**, *70*, 925–932.
- 614 (20) Simpson, S. L.; Yverneau, H.; Cremazy, A.; Jarolimek, C. V.; Price, H. L.; Jolley, D. F.
615 DGT-Induced Copper Flux Predicts Bioaccumulation and Toxicity to Bivalves in
616 Sediments with Varying Properties. *Environ. Sci. Technol.* **2012**, *46*, 9038–9046.
- 617 (21) Dabrin, A.; Durand, C. L.; Garric, J.; Geffard, O.; Ferrari, B. J. D.; Coquery, M.
618 Coupling Geochemical and Biological Approaches to Assess the Availability of
619 Cadmium in Freshwater Sediment. *Sci. Total Environ.* *424*, 308–315.
- 620 (22) Amato, E. D.; Simpson, S. L.; Jarolimek, C. V.; Jolley, D. F. Diffusive Gradients in
621 Thin Films Technique Provide Robust Prediction of Metal Bioavailability and Toxicity
622 in Estuarine Sediments. *Environ. Sci. Technol.* **2014**, *48*, 4485–4494.
- 623 (23) Amato, E. D.; Simpson, S. L.; Belzunce-Segarra, M. J.; Jarolimek, C. V.; Jolley, D. F.
624 Metal Fluxes from Porewaters and Labile Sediment Phases for Predicting Metal
625 Exposure and Bioaccumulation in Benthic Invertebrates. *Environ. Sci. Technol.* **2015**,
626 *49*, 14204–14212.
- 627 (24) Cleveland D.; Brumbaugh W. G.; MacDonald D. D. A Comparison of Four Porewater
628 Sampling Methods for Metal Mixtures and Dissolved Organic Carbon and the
629 Implications for Sediment Toxicity Evaluations. *Environ. Toxicol. Chem.* **2017**, *36*,
630 2906–2915.
- 631 (25) Parker, R.; Bolam, T.; Barry, J.; Mason, C.; Kröger, S.; Warford, L.; Silburn, B.; Sivyer,
632 D.; Birchenough, S.; Mayes, A.; et al. The Application of Diffusive Gradients in Thin
633 Films (DGT) for Improved Understanding of Metal Behaviour at Marine Disposal Sites.
634 *Sci. Total Environ.* **2017**, *575*, 1074–1086.
- 635 (26) Song, Z.; Shan, B.; Tang, W. Evaluating the Diffusive Gradients in Thin Films
636 Technique for the Prediction of Metal Bioaccumulation in Plants Grown in River
637 Sediments. *J. Hazard. Mater.* **2018**, *344*, 360–368.
- 638 (27) He, Y.; Guo, C.; Lv, J.; Hou, S.; Zhang, Y.; Zhang, Y.; Xu, J. Predicting Trace Metal
639 Bioavailability to Chironomids in Sediments by Diffusive Gradients in Thin Films. *Sci.*
640 *Total Environ.* **2018**, *636*, 134–141.

- 641 (28) Zhang, H.; Davison, W.; Miller, S.; Tych, W. In Situ High Resolution Measurements of
642 Fluxes of Ni, Cu, Fe, and Mn and Concentrations of Zn and Cd in Porewaters by DGT.
643 *Geochim. Cosmochim. Acta* **1995**, *59* (20), 4181–4192.
- 644 (29) Burton, G. A.; Greenberg, M. S.; Rowland, C. D.; Irvine, C. A.; Lavoie, D. R.; Brooker,
645 J. A.; Moore, L.; Raymer, D. F.; McWilliam, R. A. In Situ Exposures Using Caged
646 Organisms: A Multi-Compartment Approach to Detect Aquatic Toxicity and
647 Bioaccumulation. *Environ. Pollut.* **2005**, *134*, 133–144.
- 648 (30) Liber, K.; Goodfellow, W.; Den Besten, P.; Clements, W.; Galloway, T.; Gerhardt, A.;
649 Green, A.; Simpson, S. In Situ-based Effects Measures: Considerations for Improving
650 Methods and Approaches. *Integr. Environ. Assess. Manag.* **2007**, *3*, 246–258.
- 651 (31) Mann, R. M.; Hyne, R. V.; Simandjuntak, D. L.; Simpson, S. L. A Rapid Amphipod
652 Reproduction Test for Sediment Quality Assessment: In Situ Bioassays Do Not
653 Replicate Laboratory Bioassays. *Environ. Toxicol. Chem.* **2010**, *29*, 2566–2574.
- 654 (32) Belzunce-Segarra, M. J.; Simpson, S. L.; Amato, E. D.; Spadaro, D. A.; Hamilton, I. L.;
655 Jarolimek, C. V.; Jolley, D. F. The Mismatch between Bioaccumulation in Field and
656 Laboratory Environments: Interpreting the Differences for Metals in Benthic Bivalves.
657 *Environ. Pollut.* **2015**, *204*, 48–57.
- 658 (33) Simpson, S. L.; Batley, G. E. Disturbances to Metal Partitioning during Toxicity Testing
659 of Iron (II)-rich Estuarine Pore Waters and Whole Sediments. *Environ. Toxicol. Chem.*
660 **2003**, *22*, 424–432.
- 661 (34) Costello, D. M.; Burton, G. A.; Hammerschmidt, C. R.; Taulbee, W. K. Evaluating the
662 Performance of Diffusive Gradients in Thin Films for Predicting Ni Sediment Toxicity.
663 *Environ. Sci. Technol.* **2012**, *46*, 10239–10246.
- 664 (35) Wadige, C. P. M. M.; Taylor, A. M.; Krikowa, F.; Maher, W. A. Sediment Metal
665 Concentration Survey Along the Mine-Affected Molonglo River, NSW, Australia. *Arch.*
666 *Environ. Contam. Toxicol.* **2016**, *70*, 572–582.
- 667 (36) Simpson, S. L. A Rapid Screening Method for Acid-volatile Sulfide in Sediments.
668 *Environ. Toxicol. Chem.* **2001**, *20*, 2657–2661.

- 669 (37) Baldwin, S.; Deaker, M.; Maher, W. Low-Volume Microwave Digestion of Marine
670 Biological Tissues for the Measurement of Trace Elements. *Analyst* **1994**, *119*, 1701–
671 1704.
- 672 (38) Sloane, P. I. W.; Norris, R. H. Relationship of AUSRIVAS-Based Macroinvertebrate
673 Predictive Model Outputs to a Metal Pollution Gradient. *J. North Am. Benthol. Soc.*
674 **2003**, *22*, 457–471.
- 675 (39) Wadige, C. P. M. M.; Taylor, A. M.; Krikowa, F.; Lintermans, M.; Maher, W. A.
676 Exposure of the Freshwater Bivalve *Hyridella australis* to Metal Contaminated
677 Sediments in the Field and Laboratory Microcosms: Metal Uptake and Effects.
678 *Ecotoxicology* **2017**, *26*, 415–434.
- 679 (40) Warne, M. St J.; Batley, G. E.; Van Dam, R. A.; Chapman, J.; Fox, D.; Hickey, C.;
680 Stauber, J. *Revised Method for Deriving Australian and New Zealand Water Quality*
681 *Guideline Values for Toxicants*; Queensland Department of Science, Information
682 Technology, Innovation and the Arts Report: Brisbane (AU).
- 683 (41) ANZECC/ARMCANZ. Australian and New Zealand Guidelines for Fresh and Marine
684 Water Quality. *Australian and New Zealand Environment and Conservation Council*
685 *and Agriculture and Resource Management Council of Australia and New Zealand,*
686 *Canberra*. 2000, pp 1–103.
- 687 (42) Amato, E. D.; Simpson, S. L.; Remaili, T. M.; Spadaro, D. A.; Jarolimek, C. V.; Jolley,
688 D. F. Assessing the Effects of Bioturbation on Metal Bioavailability in Contaminated
689 Sediments by Diffusive Gradients in Thin Films (DGT). *Environ. Sci. Technol.* **2016**,
690 *50*, 3055–3064.
- 691 (43) Naylor, C.; Davison, W.; Motelica-Heino, M.; Van Den Berg, G. A.; Van Der Heijdt, L.
692 M. Potential Kinetic Availability of Metals in Sulphidic Freshwater Sediments. *Sci.*
693 *Total Environ.* **2006**, *357*, 208–220.
- 694 (44) Lesven, L.; Gao, Y.; Billon, G.; Leermakers, M.; Ouddane, B.; Fischer, J. C.; Baeyens,
695 W. Early Diagenetic Processes Aspects Controlling the Mobility of Dissolved Trace
696 Metals in Three Riverine Sediment Columns. *Sci. Total Environ.* **2008**, *407*, 447–459.

- 697 (45) Naylor, C.; Davison, W.; Motelica-Heino, M.; Van Der Heijdt, L. M.; Van Den Berg, G.
698 A. Transient Release of Ni, Mn and Fe from Mixed Metal Sulphides under Oxidising
699 and Reducing Conditions. *Environ. Earth Sci.* **2012**, *65*, 2139–2146.
- 700 (46) Petersen, W.; Wallman, K.; Pinglin, L.; Schroeder, F.; Knauth, H. D. Exchange of Trace
701 Elements at the Sediment-Water Interface during Early Diagenesis Processes. *Mar.*
702 *Freshw. Res.* **1995**, *46*, 19–26.
- 703 (47) Tankere-Muller, S.; Zhang, H.; Davison, W.; Finke, N.; Larsen, O.; Stahl, H.; Glud, R.
704 N. Fine Scale Remobilisation of Fe, Mn, Co, Ni, Cu and Cd in Contaminated Marine
705 Sediment. *Mar. Chem.* **2007**, *106*, 192–207.
- 706 (48) Forster, S. Spatial and Temporal Distribution of Oxidation Events Occurring Below the
707 Sediment-Water Interface. *Mar. Ecol.* **1996**, *17*, 309–319.
- 708 (49) Wadige, C. P. M.; Taylor, A. M.; Maher, W. A.; Krikowa, F. Bioavailability and
709 Toxicity of Zinc from Contaminated Freshwater Sediments: Linking Exposure-Dose-
710 response Relationships of the Freshwater Bivalve *Hyridella australis* to Zinc-Spiked
711 Sediments. *Aquat. Toxicol.* **2014**, *156*, 179–190.
- 712 (50) Wadige, C. P. M.; Maher, W. A.; Taylor, A. M.; Krikowa, F. Exposure-dose-response
713 Relationships of the Freshwater Bivalve *Hyridella australis* to Cadmium Spiked
714 Sediments. *Aquat. Toxicol.* **2014**, *152*, 361–371.
- 715 (51) Wadige, C. P. M.; Taylor, A. M.; Maher, W. A.; Ubrihien, R. P.; Krikowa, F. Effects of
716 Lead-Spiked Sediments on Freshwater Bivalve, *Hyridella australis*: Linking Organism
717 Metal Exposure-Dose-Response. *Aquat. Toxicol.* **2014**, *149*, 83–93.
- 718 (52) Wadige, C. P. M. M.; Taylor, A. M.; Krikowa, F.; Lintermans, M.; Maher, W. A.
719 Exposure of the Freshwater Bivalve *Hyridella australis* to Metal Contaminated
720 Sediments in the Field and Laboratory Microcosms: Metal Uptake and Effects.
721 *Ecotoxicology* **2017**, *26*, 415–434.
- 722 (53) Trevisan, R.; Delapedra, G.; Mello, D. F.; Arl, M.; Schmidt, E. C.; Meder, F.;
723 Monopoli, M.; Cargnin-Ferreira, E.; Bouzon, Z. L.; Fisher, A. S.; Sheehan, D.; Dafre,
724 A. L. Gills Are an Initial Target of Zinc Oxide Nanoparticles in Oysters *Crassostrea*

725 Gigas, Leading to Mitochondrial Disruption and Oxidative Stress. *Aquat. Toxicol.* **2014**,
726 *153*, 27–38.
727

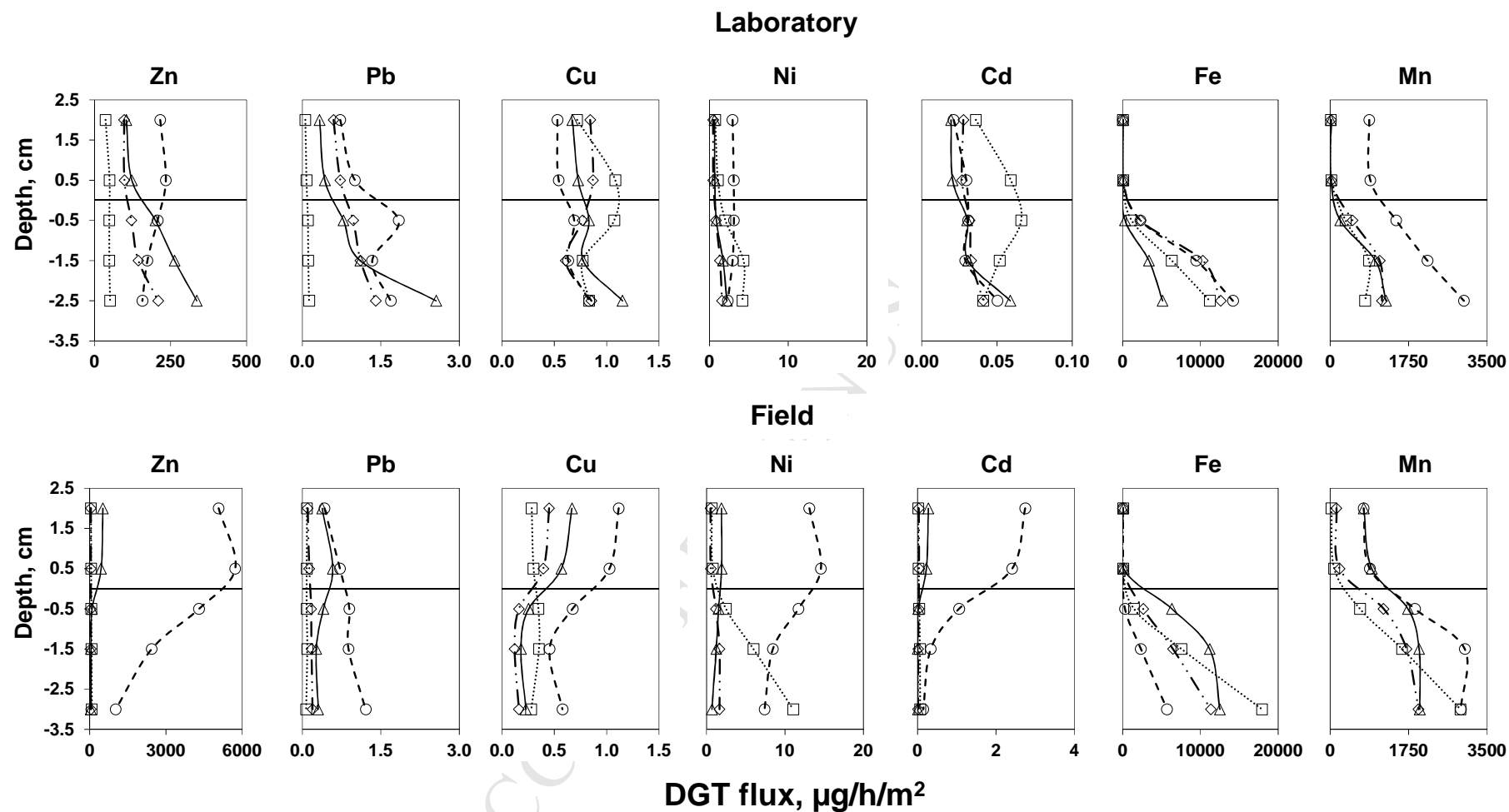
ACCEPTED MANUSCRIPT

728
729**Table 1. Physical and chemical properties of sediments and bioaccumulation in *H. australis*.**

Sediment	Total recoverable metals (TRM), mg/kg				Tissue concentration in <i>H. australis</i> (µg/g) - laboratory				AVS	Particle size
	Cd	Cu	Pb	Zn	Cd	Cu	Pb	Zn	µmol/g	< 63 µm, %
S1 (reference)	<1	10.0±0.3	16±1	95±2	0.08±0.02	4.6±0.2	2.9±0.3	258±8	<0.5	31±2.7
S2	3.2±0.1*	26.9±0.9	47.2±0.3	910±2*	0.17±0.01 ^{ab}	5.0±0.4	2.6±0.3	281±7	1.7±0.6	48±0.4
S3	1.2±0.1	26.2±0.3	33±1	840±10*	0.32±0.01 ^{ab}	5.23±0.3	2.8±0.4	297±12 ^b	<0.5	96±0.4
S4	5.3±0.1*	55.1±0.5	130±1*	2100±18*	0.31±0.01 ^{ab}	5.0±0.4	3.4±0.3	325±20 ^b	6.6±0.7	43±0.4
Sediment	Dilute-acid extractable metals (AEM), mg/kg				Tissue concentration in <i>H. australis</i> (µg/g) - field				SEM-AVS	TOC
	Cd	Cu	Pb	Zn	Cd	Cu	Pb	Zn	µmol/g	%
S1 (reference)	<1	5.9±0.1	8.9±0.2	58±3	0.07±0.02	5.5±0.5	2.7±0.2	294±15	1	1.4
S2	2.6±0.3*	4.8±0.3	37±2	790±14*	0.07±0.02 ^b	5.8±0.6	3.6±0.9	301±25	11	1.6
S3	1.0±0.1	9.0±0.2	23±1	750±33*	0.08±0.03 ^b	6.2±0.4	4.5±0.9	447±48 ^{ab}	12	4.3
S4	4.5±0.2*	5.4±0.3	106±5*	1800±80*	1.47±0.14 ^{ab}	5.1±0.6	3.4±0.3	756±42 ^{ab}	22	1.7
SQG values	1.5	65	50	200					0	

730 AVS = acid-volatile sulfide; SEM-AVS = the molar difference, where SEM is equivalent to AEM. TOC = total organic carbon and % <63 µm
731 refers to the percentage (by weight) of fine sediment particles. All concentration are mean ± SE (*n*=3). Concentrations for a greater range of
732 metals and metalloids are provided in the Table S1. Bioaccumulation data are mean ± SE (*n*=15, dry mass). The asterisk denotes concentrations
733 exceeding the sediment quality guideline values (SQG).¹ The letters 'a' and 'b' indicate statistically different bioaccumulation (see main text)
734 between bivalves exposed to the reference (S1) and contaminated sediments (S2, S3, S4), and between bivalves exposed to laboratory and field
735 conditions, respectively.

736

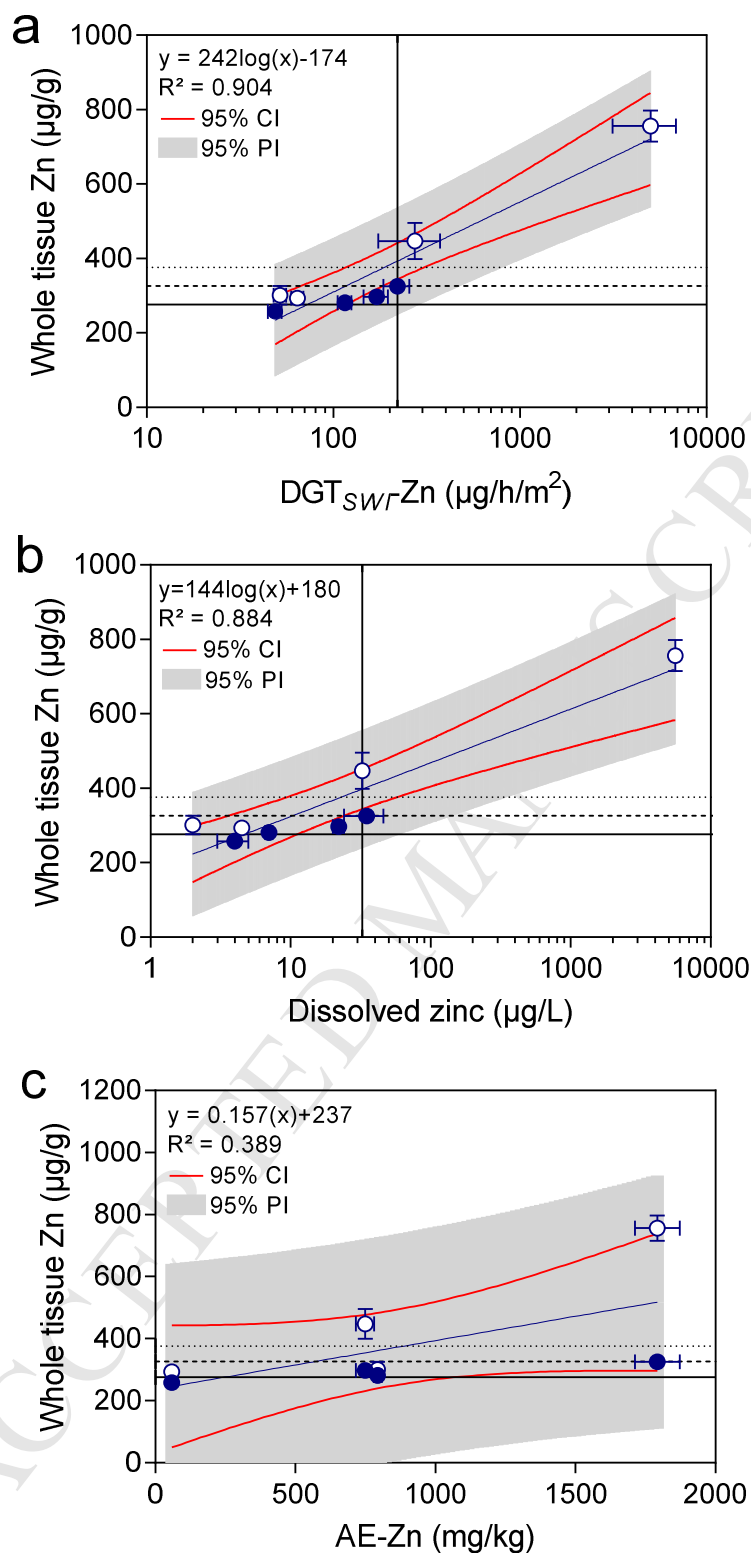


737

738 **Figure 1.** DGT profiles of Zn, Pb, Cu, Ni and Cd measured in the different sediments (S1(□), S2(◇), S3(△), S4(○),) in the laboratory and field.

739 Data points are average values of six replicates from the first and second deployments (standard deviations were ~25 and ~30% of mean values

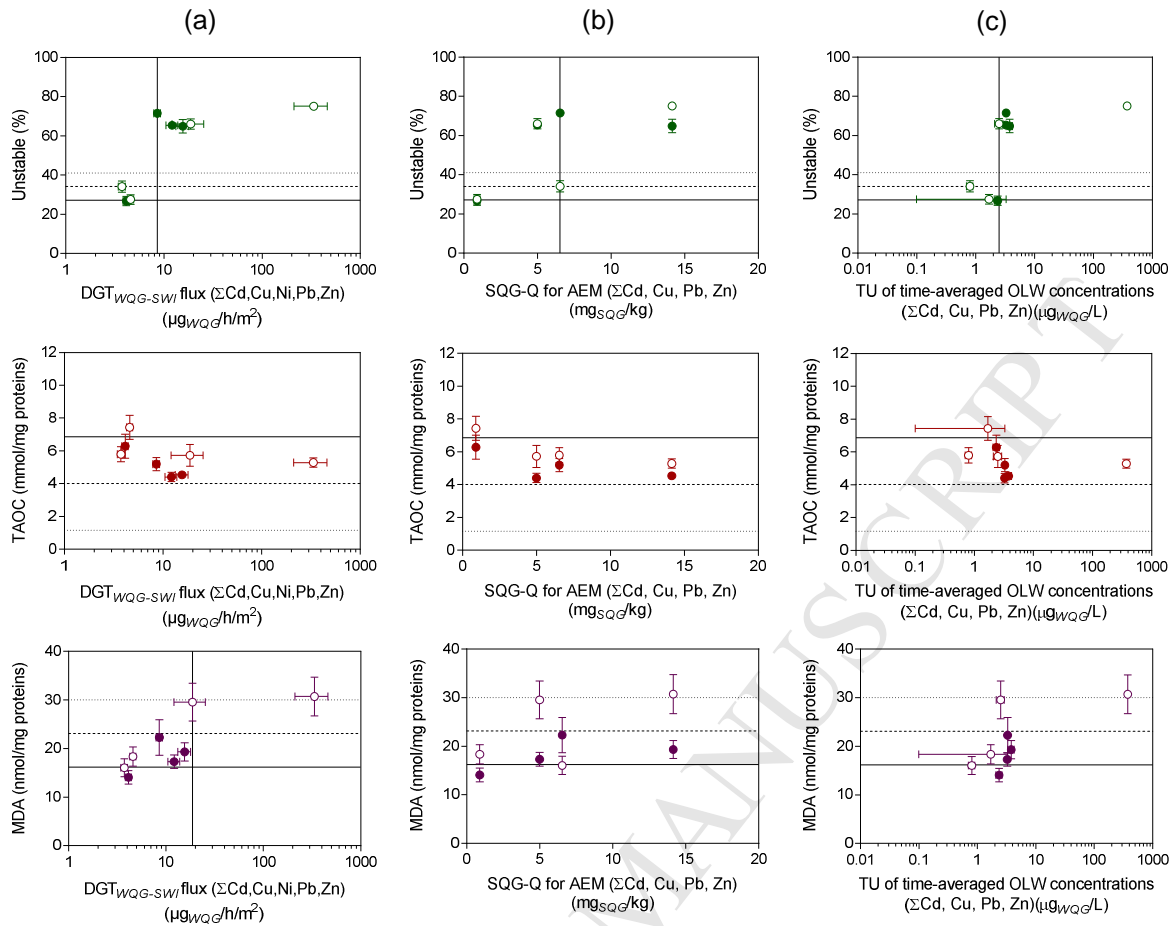
740 for laboratory and field deployments, respectively). Connecting lines are for visual aid only.



741

742 **Figure 2.** Comparison between predictions of bioaccumulation in *H. australis* obtained using
 743 (a) $\log_{DGT_{SWF}}$ -Zn flux, (b) dissolved zinc concentrations, (c) dilute-acid extractable
 744 (particulate) AE-Zn concentrations, and. Filled and open circles refer to laboratory and field
 745 deployments, respectively. Shaded areas and red lines represent the 95% prediction intervals
 746 (PI) and 95% confidence intervals (CI), respectively. The solid horizontal and vertical lines

747 separate the data into four quadrants: the solid horizontal line represents the mean
748 concentration found in bivalves exposed to control sediments (average of laboratory and
749 field), whereas the dashed and dotted horizontal lines are the mean concentration measured in
750 bivalves exposed to control sediments plus 1s and 2s, respectively; the continuous vertical
751 line corresponds to the dissolved zinc concentration, AE-Zn concentration, or DGT-Zn flux
752 above which bioaccumulation was consistently higher than the controls mean plus 1s. Data
753 points are means \pm SE (n=2, 3, 6, and 15 for dissolved zinc concentrations, AE-Zn
754 concentrations, log_DGT_{SWT}-Zn fluxes and whole tissue zinc concentrations in *H. australis*,
755 respectively).



756

757 **Figure 3.** Comparison between predictions of stress biomarker levels in *H. australis* obtained
 758 using (a) DGT_{SWI} flux normalized to WQG threshold values, (b) SQG-Q for AEM
 759 concentrations, and (c) TU of time averaged OLW concentrations. Filled and open circles
 760 refer to laboratory and field deployments, respectively. The solid horizontal and vertical lines
 761 separate the data into four quadrants: the solid horizontal line represents the mean
 762 concentration found in bivalves exposed to control sediments (average of laboratory and
 763 field), whereas the dashed and dotted horizontal lines are the mean concentrations measured
 764 in bivalves exposed to control sediments plus 1s and 2s, respectively; the continuous vertical
 765 line corresponds to the DGT_{SWI} flux, SQG-Q concentration or TU concentrations above
 766 which bioaccumulation was consistently higher than the controls mean plus 1s.

767

- Laboratory and field sediment bioassays provided different predictions of risk
- The exposure of organisms to metals differed between laboratory and field bioassays
- DGT predicted the risk of bioaccumulation and toxicity irrespective of the exposure
- *In situ* evaluation of metal bioavailability may improve sediment quality assessment